PAPER 72 (SESSION VI)

Fracture mechanics technology applied to heavy section steel structures

E. T. WESSEL, W. G. CLARK, Jr. and W. H. PRYLE

Summary

This paper presents a review of a comprehensive program initiated to assess the applicability of existing linear-elastic fracture mechanics technology and testing techniques to low to intermediate strength structural steels that are employed in heavy sections in the electrical industry. The materials involved in the program include ASTM A216 Grade WCC and A533 Grade B, Class I pressure vessel steels with minimum yield strength on the order of 40,000 and 50,000 psi, respectively as well as ASTM A469, A470 alloy steels with yield strength ranging from 75,000 to 150,000 psi. Plane-strain fracture toughness data were generated as a function of temperature for each of the alloys studied. Compact-tension types of fracture toughness specimens ranging from 1 in to 10 ins thick were involved in the program. Room temperature fatigue crack growth rate data expressed in terms of fracture mechanics parameters were also established for the A533B and A216C pressure vessel steels. The fracture toughness and fatigue crack growth rate data are used in an example problem to demonstrate the usefulness of the fracture mechanics approach to design.

Although the entire program has not been completed, sufficient progress has been made to develop the conclusion that existing linear-elastic fracture mechanics technology is applicable to low-to-intermediate strength steels when used in sufficiently heavy sections to have plane-strain conditions.

Introduction

During the past few years there has been a rapid advancement in the development and application of linear-elastic (plane-strain) fracture mechanics technology. Originally much of the work on this technology was focused on the relatively brittle, high-strength materials. As a result, it is now generally accepted that the technology, when properly employed, is a very useful quantitative tool for the prevention of failure in structures employing these high-strength materials. While most of the experience has been confined to these relatively brittle materials, there are no obvious technical reasons why the technology would not be equally applicable to the lower-strength, higher-toughness materials when employed in structures having sufficient thickness and other restraint to provide essentially plane-strain conditions.

Many of the products of the electrical industry involve heavy section structures (made of low-to-intermediate strength steels), for example, thick-walled pressure vessels, large forgings for turbine and generator rotors and disks and related thick section equipment used in power generation. The heavy sections involved have led to the basic assumption that plane-strain conditions prevail in most of these applications, at least for some portions

of the operating temperature range. Because of the high potential offered by the linear-elastic fracture mechanics technology for making quantitative, engineering decisions concerning the various aspects of fracture prevention in these applications, a broad large scale program is being conducted to assess the applicability of the technology to these situations and the associated low-to-intermediate strength materials. While the entire program is not complete, sufficient progress has been made to develop the conclusion that the technology is applicable. The currently available results of the various facets of this broad investigation are summarized in this paper.

General description of the basis of the technology

The linear-elastic fracture mechanics approach to the design against failure of structural materials is basically a stress intensity consideration in which criteria are established for fracture instability in the presence of a crack [1-3]. Consequently, a basic assumption in employing the technology is that a crack or crack-like defect exists in the structure. The essence of the approach is to relate the stress field developed in the vicinity of the crack tip to the applied nominal stress on the structure, the material properties and the size of defect necessary to cause failure.

The elastic stress field in the near vicinity of a crack-tip can be described by a single term parameter designated as the stress intensity factor 'K' [1-3]. The magnitude of this stress intensity factor in turn, is dependent upon the geometry of the body containing the crack, the size and location of the crack, and the distribution and magnitude of the external loads on the body.

Therefore, if the relationship between the stress intensity factor and the pertinent external variables (applied stress and flaw size) is known for a given structural geometry containing a particular type defect, the stress conditions in the region of the crack-tip can be established from knowledge of the applied stress and flaw size alone. The relationship between the stress intensity factor and the pertinent external variables has been established for many structural configurations and will be discussed later in this paper.

The criterion for brittle failure in the presence of a crack-like defect is that crack growth to failure (instability) will occur whenever the crack-tip stresses exceed some critical condition. Since the crack-tip stress field can be described in terms of the stress intensity factor K, a critical value of the stress intensity factor can be used to define the critical crack-tip stress conditions for failure. For the opening mode (I) of loading (tension stresses perpendicular to the major plane of the flaw) under brittle plane-strain conditions (limited crack-tip plasticity), the critical stress intensity factor for fracture instability is designated as K_{Ic}.* In addition, since the

* The subscript I is used to designate the opening mode of crack surface displacement. Subscripts II and III are used to designate shear modes of displacement. This paper deals exclusively with mode I.

localized crack-tip stresses necessary to initiate failure are material dependent, K_{Ic} can be considered a material property which represents the materials inherent resistance to failure in the presence of a crack or crack-like defect.

In view of the relationship between the stress intensity factor and the external loading variables discussed above, it becomes apparent that any combination of applied load, structural configuration and crack geometry and size which yields a stress intensity factor equal to or in excess of the critical stress intensity, K_{Ic}, for the material will result in failure. Therefore, if the appropriate stress intensity factor expression is known for a given loading configuration as well as the material's K_{Ic}, it is possible to compute either the maximum allowable stress or flaw size which will not result in the failure of the structure.

While the termination of the life of a structure or component may be based on the critical flaw size for total failure, it must be recognized that the total useful life of a cyclic-loaded component is dependent upon the rate of growth of flaws from a sub-critical size to a critical size. Therefore, both an understanding of the critical combination of stress and defect size for catastrophic fracture, and the rate of crack growth characteristics of the material under application conditions, are essential to determining the useful life of a component.

Fatigue (slow) crack propagation is a localized phenomenon dependent upon the temperature, environment, and stress conditions at the crack front. The stress intensity factor 'K' provides one of the best means available for describing the stress conditions at the tip of the advancing crack. For a given geometry (flaw and component) and given loading conditions, the crack growth rate is dependent upon the stress intensity at the tip of the crack. For given conditions, the stress intensity factor K is a function of the applied load (stress) and the crack length 'a'; that is, $K \sim \sigma \sqrt{a}$. As the crack grows under constant load cycling, the stress intensity increases since both 'a' *and* σ are increasing. Eventually the crack grows to a sufficient length that the stress intensity K increases to a level equivalent to the material characteristic K_{Ic}, the critical stress intensity factor. At this point, brittle fracture (crack instability) occurs.

Slow crack growth can also occur under conditions of sustained loading (constant load with time), particularly in the presence of a hostile environment. In such cases it is also essential to have materials properties data in the form of da/dt (change in crack length per unit time) as a function of the stress intensity factor, K_I.

In the presence of sustained loading in a hostile environment, such as sea water, it is generally believed that there is a threshold level of K_I (designated as K_{ISce} for the critical stress intensity factor for stress-corrosion cracking), below which a crack will not grow. The K_{ISce} parameter, a constant for a given material and environment, is therefore another material

parameter of interest where hostile environments may prevail. Realistically, this K_{ISCC} threshold level should also be qualified as being applicable for a specific time period.

Fracture mechanics material parameters for low-to-intermediate strength structural steels

Test methods

One of the foremost factors which has thwarted the use of fracture mechanics for the lower strength materials has been the experimental difficulty in obtaining the necessary fracture mechanics parameters, particularly the K_{Ic} fracture toughness. Nearly any of the fracture mechanics types of fracture toughness tests [4, 5] that have been successfully used to obtain K_{Ic} for the relatively brittle, high-strength materials could also be used for the lower-strength steels, provided a sufficiently large specimen to maintain the required degree of plane-strain conditions is used [4-7]. For most of the steels of interest to the electrical industry, the yield strength-toughness combination (K_{Ic}/σ_{YS}) is such that the common types of specimens would have to be so large that they are practically prohibitive. Early efforts in the program, then, were centered on the development of a suitable specimen for the measurement of K_{Ic}. This work has resulted in the development of a relatively small specimen [6, 8] for determining K_{Ic} in the lower yield-strength, high-toughness materials of interest. The proposed ASTM recommended test method [8] for determining K_{Ic} now incorporates a 'compact-tension' type of specimen. The K_{Ic} data reported in this paper were obtained with the compact tension type of specimen and the ASTM recommended test procedure [5, 6, 8]. Additional data have been obtained using the spin burst test [9].

Fig. 1 provides the geometry and general proportions of the compact tension specimen and lists the measurement capacities of several sizes of specimens.* Actual specimens of 1 in, 2 in, 4 in, 6 in and 12 in thickness are shown in Fig. 4.

Crack growth rates can be obtained with the same types of specimens as are used for K_{Ic} determinations, providing the K_I calibration extends over a suitable range of crack lengths and an appropriate crack length monitoring system is employed. Most of the crack growth rate data obtained in this program and reported in this paper were obtained using the modified WOL-T* type of geometry [6] and the methods developed by Clark [10]. An automatic crack extension monitoring system [11] is used to get basic 'a' vs N data (crack length versus cycle), and the resulting da/dN vs ΔK_I (crack growth per cycles as a function of the applied stress intensity factor range) relationships were determined with an appropriate computer program [12].

* Note that the number preceding the Specimen Identification Code (CT, WOL) refers to the specimen thickness.

K_{Ic} fracture toughness data

Some of the K_{Ic} toughness data obtained for typical low-to-intermediate strength steels are described below. These are: ASTM A533 Grade B steel (50,000 psi minimum yield strength) commonly used for large welded pressure vessels; ASTM A216C cast steel (40,000 psi minimum yield strength), also used for thick pressure vessels; and ASTM A469, A470 and A471 alloy steels employed for large generator-turbine rotor and disk forgings at yield strengths ranging from 75,000 psi to 150,000 psi. The chemical composition, heat treatment and conventional mechanical properties are provided in Figs. 3 and 4.

The temperature dependence of K_{Ic} fracture toughness for a 12 in thick A533B steel plate is shown in Fig. 5.* For convenience, the yield strength is also shown. All of these fracture toughness data are valid plane-strain K_{Ic} measurements according to the ASTM Committee E-24 recommended criterion [4-8]. Additional tests of various size specimens were also conducted but these results did not suffice the recommended size criteria (crack length 'a' and thickness 'B' $\geqq 2{\cdot}5\,(K_{Ic}/\sigma_{YS})^2$, hence these data are not included in Fig. 5. All test specimens were taken from a single, large 12 in thick plate and were oriented such that the fracture plane was in the width and thickness direction of the plate; thus the direction of fracture propagation was normal to the primary rolling direction of the plate. The loading rate was $K = 100$ ksi $\sqrt{\text{in}}$ per min, corresponding to a slow (static) loading. In all cases the center of the specimen thickness correspond to the center of the plate thickness. Conventional transition temperatures are also shown.

As may be seen in Fig. 5 several sizes of specimens were used, the size increasing with increased test temperature. This is necessary in order to maintain plane-strain conditions in the tests as the K_{Ic} toughness increases and yield strength decreases with increased temperature. Of particular significance in Fig. 5 is the rapid increase in K_{Ic} which occurs in the temperature range between 0°F and room temperature. As will be demonstrated in a subsequent section of this paper, the high level of K_{Ic} fracture toughness at ambient temperatures permits the existence of high stresses and very large defects without resulting in failure.

Other thick plates of A533B steel have also been investigated. The K_{Ic} fracture toughness of one of these is shown in Fig. 6. The specimen size in this plate was limited to 4 in thick; hence valid data were not obtained

* Appreciation is expressed to T. R. Mager of the Pressurized Water Reactor Plant Division of W. Electric Corp. for permission to use the results of the 1 in and 2 in thick specimens. These tests, from the same plate as the large specimens, are a portion of related programs sponsored under a joint Westinghouse Electric Corporation–Empire State Atomic Development Associates agreement and with the cooperation of the Oak Ridge National Laboratories, Heavy Section Steel Technology Program.

to as high temperatures as were attained with the large specimens in the other plate (Fig. 5). The effect of specimen orientation (transverse versus longitudinal) were also studied (Fig. 6) and no significant effect was observed for this plate which had received a high degree of cross-rolling. In general the fracture toughness of the two heavy plates (Figs. 5 and 6) are quite comparable.

These data (Figs. 5 and 6) for base plate of A533B steel are only a preliminary portion of the data being accumulated in the over-all program on this steel. The K_{Ic} fracture toughness test program is continuing and incorporates additional tests for evaluating welds and heat-affected-zones, and temperature and loading rate effects. A parallel program on the effects of irradiation is also being conducted.* When all of these data are available, it will be possible to conduct complete, quantitative evaluations of all aspects of pressure vessel design, fabrication and operation, using sophisticated fracture mechanics technology.

The K_{Ic} fracture toughness of the three classes of forging steels used in generator and turbine rotors are summarised in Fig. 7. These data represent the results obtained in a large program involving several forging for each class of steel. Several types and sizes of compact tension, as well as spin burst tests [9] were employed to obtain these data, and this program has been reported in detail [13]. As was true for the A533B steel, the forging steels also exhibit a relatively rapid rise in K_{Ic} fracture toughness in the temperature range of practical interest.

Some of the auxiliary pressure vessels utilized in electrical power generation employ thick walled steel castings, commonly ASTM A216. These steels are generally of a lower yield strength than the primary pressure vessel (A533B) and forging steels described above. Because of the very thick walls (8-10 in) of these castings, it appeared possible that linear elastic fracture mechanics may also be applicable to these steels in spite of their relatively low strength [14]. Some K_{Ic} fracture toughness data have been obtained for these steel castings using thick compact tension specimens. Some typical results are shown for A216C cast steel in Fig. 8. Specimens up to 8 in thick were employed, but even with this thickness the material was too tough (too much crack-tip plasticity prior to fracture) to provide plane-strain conditions in tests in the temperature range of practical interest. Additional tests using even larger specimens (up to 12 in thick) are currently being conducted in an effort to extend the valid K_{Ic} data to higher temperatures than those obtained with the 8 in specimens (Fig. 8). Although the data of Fig. 8 do not extend to as high temperatures as may be desired, the data are still very useful in evaluating fracture potential as will be described in the next section of this paper.

* Programs being conducted by the Pressurized Water Reactor Plant Division of the Westinghouse Electric Corp., Pgh., Pa., a portion of which is sponsored under a USAEC-EURATOM Joint Research and Development Program.

Crack growth rate data

While a knowledge of the K_{Ic} fracture toughness and the nominal stresses prevailing in the component is adequate for describing the critical conditions of defect size for the termination of life, we must also have crack growth rate data for describing and controlling the sequence of events leading to total failure under cyclic loading conditions. The program has developed appropriate crack growth rate data for use in the sub-critical crack growth considerations for the same applications and materials described in the previous section of K_{Ic} toughness.

The crack growth rate characteristics of ASTM A533B steel plate under cyclic loading are being determined, including the effects of such variables as temperature, specimen size, direction and plane of propagation, location within the thickness of heavy plate, water environment, cyclic frequency, etc.* This portion of the program is still in progress. Additional tests are being conducted to confirm the preliminary results, as well as investigations including weld metals and heat-affected-zone, and higher temperature data (~550°F). However, sufficient data are currently available [15] to illustrate some of the basic aspects of the crack growth behavior in A533B steel, and its general application to fracture prevention considerations.

Some representative data from this program illustrating the general crack growth rate characteristics of A533B plate at room temperature are provided in Fig. 9 in terms of the crack growth rate da/dN as a function of the stress intensity range, ΔK_I. The parameters identified as n and C_o represent empirical material constants established as a result of analyzing the growth rate data in terms of the generalized exponent fatigue crack growth rate law [16]: $da/dN = C_o K^n$. The ΔK_I parameter is the stress intensity range applied during the cycle of loading, n is the slope of the log da/dN versus log ΔK_I curve and C_o is the intercept constant. From a knowledge of these parameters, as well as knowing the critical defect size for total failure, it is possible to compute the number of elapsed cycles required to cause failure for a variety of initial defect sizes, component geometries, and loading conditions. A convenient cyclic life expression based on fracture mechanics principles and using the above parameters has been developed by Wilson [17], and employed by others [2]. The practical use of these data and expressions is illustrated in the next section of the paper.

The preliminary results currently available relative to environmental effects indicate that there are no effects of water on either the crack growth rates in the A533 steel, either under cyclic or sustained loading. Hence no values for environmental enhanced cyclic crack growth rates or K_{ISce} can be reported, nor is it necessary to factor environmental considerations into the subsequent example problems.

* Sponsored by Pressurized Water Reactor Plant Division of Westinghouse Electric Corporation in cooperation with Empire State Atomic Development Associates—cognizant engineer T. R. Mager.

Cyclic crack growth rate data have been obtained for several low-strength A216 steel castings of various quality and containing various degrees of both microscopic and macroscopic defects. In general the growth rate characteristics were observed to be relatively consistent, particularly when the influence of gross defects are properly accounted for. Some representative data from this investigation are provided in Fig. 10. These data are from the same casting as employed for K_{Ic} measurements given in Fig. 8. These crack growth rate data will be used in conjunction with the corresponding K_{Ic} data in the example problems which follow.

The other materials parameter essential to the use of the fracture mechanics technology is the conventional engineering yield strength (0·2% offset) as measured in the service metallurgical conditions and at the temperatures and strain rates of interest. These data were accumulated as a portion of the K_{Ic} fracture toughness test program and the results are given in the corresponding K_{Ic} temperature graphs (Figs. 5, 6, 7, 8).

Application of fracture mechanics technology

General use of the technology

The general principles and use of the fracture mechanics technology can best be illustrated from the point of view of considering the fracture sequence and the various critical sizes of defects involved in the fracture processes. Fig. 11 provides a schematic representation of the fracture process and the defects of interest. By using a K_I expression appropriate to the geometry of interest, and knowing the flaw size and nominal stress in the vicinity of the flaw, an instantaneous K_I level can be determined for any point in the fracture process. Thus at the start of life (Stage 1), by using the applied stress and the flaw size initially present in the component, an initial K_I level, K_{Ii} is defined. For practical purposes the flaw size associated with this K_{Ii} level must be larger than that definable by the nondestructive inspection capability. Under normal operating conditions this initial flaw can grow under cyclic and/or sustained loading. As the crack grows and the load on the component remains constant, the K_I level increases. The rate of growth is defined by the da/dN, ΔK_I relationship. In situations where a hostile environment is present and where the material has a K_{ISce} value which is less than K_{Ic}, the crack will grow, at a rate defined by the normal da/dN versus K relationship, until the K_I level becomes equivalent to K_{ISce}, Stage 2. The amount of growth between stages 1 and 2 will be dependent upon the relative difference in the K_{Ii} and the K_{ISce} level of stress intensity and the material characteristics. At Stage 2 the flaw will start to grow faster than the normal rates due to the action of the hostile environment and the existence of a K_I level above the threshold, K_{ISce}. Accelerated flaw growth will continue to occur until the K_I level reaches K_{Ic}, at which point total rapid fracture will occur, Stage 3. In cases

where there are no environmental effects, Stage 2 is absent and the fracture sequence passes directly from Stage 1 to Stage 3. This latter sequence will be used in the example problems.

In practical considerations it is desirable that the material must have adequate K_{Ic} fracture toughness, K_{ISce} corrosion resistance, and resistance to crack growth to permit the existence of flaws of a discernible size and still provide (with appropriate safety factors) the desired life and integrity in the component. Alternatively, if an appropriate material is not available, the design stresses must be reduced to a level where flaws of an inspectable size can exist without endangering the integrity of the component. Referring to Fig. 11 the K_{Ic} fracture toughness and subcritical crack growth rate characteristics must be such that the initial flaw that could be present at the start of life and still have satisfactory performance is well within the limits of the inspection techniques that can be practically applied. The specifications and acceptance limits should be set at a flaw size which is somewhere between the inspection capability and the initial flaw size (Stage 1). This will provide assurance that flaws of a size equivalent to Stage 1 'K_{Ii}' will not exist in the structure, and at the same time will provide an additional safety factor on life. That is, considerable additional life, beyond that allowed for going from Stage 1 to Stage 3, will be gained by the fact that the flaw will first have to grow from the acceptance limits to Stage 1. Since, the size of the flaw will be relatively small, the K_I level will be relatively low; hence the rate of growth will be slow during this period (see data for low ΔK_I in Figs. 9, 10). Additional safety factors on life can also be applied relative to the growth from Stage 1 to Stage 3. Using fracture mechanics, quantitative values can be assigned relative to these safety factors as will be demonstrated in an example problem later in the paper.

The same type of reasoning described above can also be applied to situations where a defect is discovered during service and it is then necessary to make some quantitative judgments relative to the remaining life. Should the component be taken out of service and repaired or replaced, or can it be operated safely for some continued period of time? How close are the existing conditions to terminal failure [7]. With appropriate information concerning the K_I expression for the geometry of concern, the prevailing stresses, the defect size, and the material characteristics, the above types of questions can be answered in a quantitative fashion using fracture mechanics. Naturally the degree of quantitativeness will depend upon the preciseness of the information that is available. For purposes of engineering judgments, approximate information is often sufficient.

Specific examples of the application of fracture mechanics technology

The foregoing section has dealt with the generalised use of the fracture mechanics technology. This section is intended to provide some specific

examples relative to the types of applications involving low-strength, intermediate to high-toughness materials such as those described previously in this paper. It will not be possible to include all of the considerations that can be and are employed in these areas of application but some of the more pertinent aspects will be described in detail.

For example purposes, let us limit our discussion to large pressure vessel applications involving the A533-B plate and A216-C cast steels for which fracture mechanics data were presented earlier. In addition, let us assume room temperature loading conditions in a non-hostile environment. To further simplify the example, we will confine our discussion to one defect geometry which represents a worst case flaw geometry, that is, a semi-eliptical surface flaw with a length to depth ratio of 10 or more. The following examples will also be confined to surface defects on the outside of the uniform cylindrical body of the pressure vessel oriented such that the major plane of the flaw is perpendicular to the primary stresses (hoop stresses). Wherever possible, the stress conditions used in the examples were established in accordance with the ASME Boiler and Pressure Vessel Code Section III (1968). For simplification purposes, possible residual stresses from fabrication are assumed to be negligible.

The example problems illustrate three basic areas of concern common to most design considerations: proof testing, service operating conditions including cyclic life, and the development of material acceptance and inspection criteria. The fracture mechanics approach to evaluating each of these areas is described in detail.

Proof testing

One of the crucial periods in the early life of pressure vessels occurs during the proof test which is usually conducted before a vessel goes into service. From a knowledge of the material properties and stresses prevailing in the structure during the proof test, it is possible to calculate the critical size of defect which could cause failure during the test. This information can then be used to evaluate the adequacy of the material properties and the nondestructive inspection procedures that were employed. Alternatively this type of analyses can be employed to establish the material and inspection requirements prior to fabrication of the vessel. In addition, the critical flaw size data associated with proof test conditions can also be used for life expectancy considerations. Specifically, if a pressure vessel survives a given proof test it can be concluded that the largest defect present in the structure is smaller than the critical flaw size at the proof test conditions. Therefore, in the absence of adequate nondestructive inspection techniques, this flaw size would be considered the existing flaw size at the beginning of life at the operating conditions and would in turn, serve as the basis for further crack growth considerations [18].

The following discussion describes the techniques used to compute critical flaw sizes for A216-C and A533-B steels under various proof testing conditions.

The ASME Boiler and Pressure Vessel Code (Section III, 1968) limits the pressures to values which in turn limit the primary membrane stresses. Similar limitations are also placed on the combined primary membrane plus primary bending stresses. There are three possible conditions for proof tests, depending upon the specific application involved. These include hydrostatic testing at:

(1) 1·25 times the design pressure

(2) a pressure where the general membrane stresses do not exceed 0·9 times the material yield strength (σ_{YS})

(3) a pressure where the primary membrane and primary bending stresses do not exceed 1·35 times σ_{YS}.

The code also specifies the minimum allowable yield strength and maximum allowable primary membrane stress for pressure vessel steels. The specified minimum yield strength for A216-C cast steel and A533-B plate are 40,000 and 50,000 psi, respectively. The maximum allowable primary membrane stress is 23,300 psi for A216-C cast steel and 26,700 psi for A533-B plate. From this information we can establish three realistic proof test stress levels for use in the example problem.

These stress levels are summarized below:

Proof test conditions	*Proof testing stress (psi)*	
	A216-C	*A533-B*
1·25 × design pressure	29,100	33,300
0·90 × σ_{YS}	36,000	45,000
1·35 × σ_{YS}	54,000	67,500

In order to compute the critical flaw sizes for the proof test loading conditions presented above we must have K_{Ic} data for the temperature of interest, as well as the appropriate stress intensity expression for the component geometry and type of defect. Assuming that proof testing will be conducted at room temperature in a non-hostile environment, the necessary K_{Ic} data for the A533B and A216-C steels can be taken from Fig. 5 and Fig. 8, respectively. The extrapolated room temperature fracture toughness of A216-C cast steel is 155 ksi$\sqrt{\text{in}}$ and the actual toughness of A533-B steel is 130 ksi$\sqrt{\text{in}}$.

The appropriate stress intensity expression for a pressure vessel containing a long shallow surface defect perpendicular to the primary hoop stress is

$$K_I^2 = \frac{1{\cdot}21\ a\ \pi\ \sigma^2}{\phi^2 - 0{\cdot}212\ (\sigma/\sigma_{YS})^2}$$

where K_I = nominal stress intensity factor, ksi$\sqrt{\text{in.}}$
ϕ = flaw shape parameter
a = crack depth, ins
σ = applied tensile stress, ksi
σ_{YS} = 0·2% yield strength, ksi

Rearranging the above expression and setting K_I equal to K_{Ic} yields the following critical flaw size expression:

$$a_{cr} = \frac{K_{Ic}^2\ [\phi^2 - 0{\cdot}212\ (\sigma/\sigma_{YS})^2]}{1{;}21\ \pi\ \sigma^2}$$

In order to facilitate the use of this expression and specifically, to simplify the calculation of the flaw shape parameter, a graphical solution of ϕ^2 is available [19] where the flaw shape parameter is expressed as a Q factor and $Q = \phi^2 - 0{\cdot}212\ (\sigma/\sigma_{YS})^2$. The critical flaw size expression now becomes

$$a_{cr} = \frac{K_{Ic}^2\ Q}{1{\cdot}21\ \pi\ \sigma^2}$$

Solving this equation, using the room temperature K_{Ic} values and proof test stresses presented above, yields the critical flaw sizes necessary to cause failure under proof testing loading conditions.* The proof test critical flaw sizes for the A216-C and A533-B steels are summarized in Fig. 12. Note that for both materials the critical flaw sizes at the proof test condition examined are well within the limits of existing nondestructive inspection procedures. Defects of the magnitude shown in Fig. 12 normally do not exist, or would not be permitted, in actual situations. If it were to become necessary to evaluate a situation involving such large defects, considerations would have to be given to the possible effects of the large defects on the nominal stresses existing in the region of the defect.

Operating conditions

A thorough evaluation of the operating conditions associated with a specific application involving cyclic loading requires the determination of the critical flaw size as well as the initial flaw size which will grow to the critical

* For condition 3 (page 34) where the allowable pressure is equivalent to $1{\cdot}35\sigma_{YS}$ for primary membrane plus primary bending stresses, a conservative assumption is employed. That is, for purposes of the critical flaw size computations, the mean stress is taken to be $1{\cdot}35\ \sigma_{YS}$.

size during the desired life of the structure. The following examples demonstrate how these data are obtained.

Again using the ASME Code as a guideline for selecting realistic stresses for example purposes, let us assume that the maximum operating stress for our hypothetical pressure vessels will be equivalent to the maximum allowable primary membrane stress for the respective materials (23,300 psi for A216-C steel and 26,700 psi for A533B steel). In addition, let us consider a local loading situation where the maximum operating stress is 1·5 times the allowable primary membrane stress. This condition results in a maximum operating stress of 35,000 psi for the A216-C cast steel and 40,000 psi for the A533-B steel.

The critical flaw sizes associated with the assumed service conditions outlined above are computed in exactly the same manner as those obtained for proof testing. Specifically, the appropriate K_{Ic} and applied stress data are substituted into the critical flaw size expression and the expression solved for a_{cr}. Fig. 13 summarizes the critical flaw size data for the hypothetical loading conditions. These flaw sizes represent the defect size necessary to cause failure as the result of a single application of load at the prescribed operating conditions.

Cyclic life

Once the critical flaw size for the proposed operating conditions has been determined, we can proceed to the calculation of the number of cycles required for an existing flaw to grow to the critical flaw size and thus cause failure. For the purpose of our example, we will assume that the pressure vessels are cycled from essentially zero stress to the maximum operating stress. In addition, we will develop generalized cycle life curves rather than data applicable to some designated desired life conditions.

In order to calculate quantitative cyclic life data we must have suitable fatigue crack growth rate data expressed in terms of fracture mechanics parameters. Such data are available [14, 15] for the A533B and A216-C steels being considered and are given in Figs. 9 and 10 where da/dN is the crack growth rate and ΔK is the change in stress intensity factor per cycle of loading. The parameters identified as n and C_0 represent the slope of the log da/dN versus log ΔK_I curve and the intercept constant, respectively. These parameters are considered empirical material constants which describe the fatigue crack growth rate properties of the material in terms of the generalized fatigue crack growth rate law: $da/dN = C_0\ \Delta K^n$. From knowledge of these parameters, as well as the critical defect size, it is possible to compute the number of elapsed cycles required for any size of existing flaw to grow to failure.

A convenient cyclic life expression based on fracture mechanics concepts has been developed by Wilson [17] and will be used for our example

problem calculations. The general form of the equation is presented below:

$$N = \frac{2}{(n-2)\, C_0\, M^{n/2}\, \Delta\sigma^n} \left[\frac{1}{a_i^{(n-2)/2}} - \frac{1}{a_{cr}^{(n-2)/2}} \right] \text{ for } n \neq 2$$

$$N = \frac{1}{C_0\, M\, \Delta\sigma^2} Ln \frac{a_{cr}}{a_i} \text{ for } n = 2$$

where:

N = number of cycles to grow to critical flaw size (failure)
a_i = initial crack size, inch
n = slope of log da/dN versus log ΔK curve
a_{cr} = critical flaw size, inch
C_0 = empirical intercept constant
$\Delta\sigma$ = applied cyclic load range, ksi
M = component geometry and flaw shape parameter

The above expression is applicable to those loading situations where the relationship between applied load, flaw size and stress intensity factor has the form of $K_I = \sigma\sqrt{Ma}$. In addition, it is assumed that the cyclic stress range ($\Delta\sigma$) remains constant throughout the component life and that the mean stress does not influence the results.

The first step in the use of the cyclic life expression is to establish the component geometry and flaw shape parameter, M. For the problems under consideration (an elliptical surface flaw subjected to tension stresses normal to the major plane of the flaw), $K_I^2 = 1{\cdot}21\ \pi\sigma^2 a/Q$. Converting this equation to the generalized form of $K = \sigma\sqrt{Ma}$ yields $M = 1{\cdot}21\ \pi/Q$ where Q is the flaw shape parameter. We now have all the necessary parameters required to proceed with the calculation of cyclic life. The pertinent parameters for A216-C and A533-B steel at the two operating conditions under consideration are summarized below.

Material	$\Delta\sigma$	a_{cr}	C_0	n	M
A216-C Cast Steel	23,300 psi	12·2	$2{\cdot}3 \times 10^{-9}$	3	3·62
	35,000 psi	4·92	$2{\cdot}3 \times 10^{-9}$	3	3·96
A533-B Steel	26,700 psi	6·57	1×10^{-15}	2·2	3·62
	40,000 psi	2·67	1×10^{-15}	2·2	3·96

Since our objective in this portion of the example problem was to develop generalized cyclic life data for both materials at two operating (stress) conditions rather than to compute the initial allowable flaw size for some predetermined cyclic life we must solve the above cyclic life expression for a variety of initial flaw sizes thus yielding a cyclic life curve of initial flaw size versus number of cycles to failure. We arbitrarily selected as a starting point an initial flaw size 0·250 in deep and took convenient intervals of crack size up to the critical flaw size for the respective loading conditions. The resulting cyclic life curves for the A216-C and A533-B steels are presented in Figs. 14 and 15, respectively. These data represent the most convenient form of presenting cyclic life data for a specific application. From cyclic life data presented in this manner it is possible to establish quantitative material acceptance and inspection requirements as well as realistic safety factors for various practical situations where a given life and safety factor is desired.

Development of inspection requirements and safety factors

The employment of adequate nondestructive inspection criteria and design safety factors for a structure assumed to contain defects are closely related. Specifically, design safety factors for such components can be established on the basis of applied stress or cyclic life which in turn, influence the defect size that must be detectable. From cyclic life data such as that presented in Figs. 14 and 15 it is possible to readily evaluate the interrelationship between flaw size, applied stress and cyclic life for a given application.

For exmaple, if an A533-B steel pressure vessel is designed to operate at a maximum applied hoop stress of 26,700 psi for 10,000 cycles the initial allowable surface crack depth is 5·00 in and the nondestructive inspection level must be adjusted accordingly. If a safety factor of 1·5 on stress is incorporated into the design consideration, the nondestructive inspection must be adjusted to detect surface flaws 1·4 ins deep. At this inspection level the number of cycles required to cause failure at the actual operating conditions becomes 60,000; a safety factor of 6 on life. Conversely, if a safety factor of 3 on cyclic life is incorporated into the design considerations, the nondestructive inspection level must be adjusted to detect surface cracks 2·8 ins deep. Data such as that shown in Figs. 14 and 15 can also be used to compute the remaining life of a structure in which a defect has been detected after some time in service. It may also be used in conjunction with the proof test to estimate life. If, in the absence of suitable inspection techniques, the size of the initial defect is assumed to be just slightly smaller than the critical size which would have caused failure in the proof test, the cyclic life between the proof test and end of service life can be taken from Figs. 14-15. The life is that required to grow from the proof test critical size to the operating critical size.

Discussion of example problems

Consideration of the critical flaw sizes for both the proof testing and operating conditions described above clearly indicates that relatively large flaws are required to cause failure. In addition, at the lower stress levels the critical elliptical surface flaw depth approaches or exceeds the section thicknesses commonly employed in large pressure vessels. Consequently, it appears that a leak-before-failure situation could exist. To substantiate this behavior it becomes necessary to consider the case of a through-the-thickness cracked plate subjected to tension loads perpendicular to the major plane of the crack. If this flaw length necessary to cause catastrophic failure is twice the plate thickness, then generally a leak before failure condition prevails [2]. The appropriate stress intensity expression for a through-cracked plate is:

$K_I = \sigma\sqrt{\pi a}$ where σ is the applied stress and 'a' is the half crack length. As an example, solving this equation for the case of a 10 in thick wall A216-C pressure vessel subjected to the maximum code allowable stress (23,000 psi) yields a critical flaw length 2a of 28·2 ins, which is more than sufficient to provide a leak before failure situation. A similar approach can be used to evaluate the possibility of a leak-before-failure for other materials and section thicknesses.

The cyclic life data presented in Figs. 14 and 15 also illustrate that relatively large initial flaw sizes are required to cause failure in less than 100,000 cycles at a cyclic load range equivalent to the maximum allowable stress. At stresses equivalent to 1·5 times the code allowable, the initial flaw size necessary to cause failure in 10,000 cycles are also well within the current nondestructive inspection limits. At operating stress levels below the maximum code allowable and with less critical flaw geometries, the cyclic life of A533B and A216C vessels are much greater than that illustrated in our examples. Therefore, the data presented in Figs. 14 and 15 can be considered a conservative estimate of cyclic life. More realistic data for a specific pressure vessel design and a given set of operating conditions can be developed using the same procedures illustrated here.

Conclusions

Existing fracture mechanics technology is directly applicable for fracture prevention control in structures where low-to-intermediate strength steels are used in sufficiently heavy sections to promote the existence of plane-strain conditions. The technology provides the basis for quantitative evaluations of the interactions between design, materials, fabrication, and inspection, and of their cumulative effect upon the integrity and performance of the product. Proper consideration of these factors, coupled with appropriate information, can be developed into an overall fracture control plan which will ensure the desired level of integrity for the desired lifetime of the product.

Acknowledgements

The authors wish to acknowledge the contributions of their many associates at the Westinghouse Research Laboratories who contributed to various phases of this program. Particular appreciation is expressed to Messrs. L. J. Ceschini, A. J. Bush, L. M. Piraja, R. B. Stouffer, J. Malley, T. Clements and J. A. Fratangelo of the Materials Testing and Evaluation Laboratory and Messrs. W. K. Wilson and R. R. Hovan, Mechanics Department. Further appreciation is expressed to the management of the Westinghouse Research Laboratories and the various Westinghouse operating divisions for their continued interest and support of this work.

References

1. IRWIN, G. R. 'Fracture mechanics', *Structural Mechanics*, Pergamon Press, New York City and London, 1960.
2. IRWIN, G. R., KRAFFT, J. M., PARIS, P. C. & WELLS, A. A. 'Basic Aspects of crack growth and fracture', NRL Report 6598, Nov., 1967.
3. Fracture toughness testing and its applications, *ASTM STP*, p. 381, April, 1965.
4. Plane strain crack toughness testing of high strength metallic materials, *ASTM STP*, p. 410, January, 1967.
5. Proposed recommended practice for plane-strain fracture toughness testing of high-strength metallic materials using a fatigue-cracked bend specimen, *ASTM Standards*, Part 31, p. 1018, 1968.
6. WESSEL, E. T. 'State of the art of the WOL specimen for K_{Ic} fracture toughness testing', *Engineering Fracture Mechanics*, vol. 1, no. 1, p. 77, June, 1968.
7. SRAWLEY, J. E., JONES, M. H. & BROWN, W. F., Jr. 'Determination of plane strain fracture toughness', *ASTM Mtls. Res. & Stds.*, vol. 7, no. 6, pp. 262-266, June, 1967.
8. Method of test for plane-strain fracture toughness of metallic materials, Approved by ASTM Committee E24 for publication in ASTM Standards, Part 31, 1969.
9. SANKEY, G. O. 'Spin tests to determine brittle fracture under plane-strain', Paper 1356, presented at 1968 SESA Spring Meeting, Albany, N.Y., May 10, 1968, to be published *Jl. of Experimental Mechanics*, 1968.
10. W. G. CLARK, Jr., 'Ultrasonic detection of crack extension in the WOL type fracture toughness specimen', *Materials Evaluation*, p. 185, August, 1967.
11. CLARK, W. G., Jr. & CESCHINI, L. J. 'An ultrasonic crack growth monitor', Westinghouse Research Laboratories Scientific Paper No. 68-7D7-BFPWR-P1, April, 1968, to be published.
12. FEDEROWICZ, A. J. & POWELL, B. A. 'A computer program to obtain a min-max regression model by linear programming', Being prepared for publication.
13. GREENBERG, H. D., WESSEL, E. T. & PRYLE, W. H. 'Fracture toughness of turbine-generator rotor forgings', Presented at 2nd National Conference on Fracture Mechanics, Lehigh Univ., Bethlehem, Pa., June, 1968, To be published in Engineering Fracture Mechanics, 1969.
14. GREENBERG, H. D. & CLARK, W. G., Jr., 'A fracture mechanics approach to the development of realistic acceptance standards for heavy walled steel castings', presented at the ASM Metal Congress Detroit, October, 1968. To be published by ASM.
15. BATES, R. C. & CLARK, W. G., Jr. 'Fractography and fracture mechanics', Presented at ASM Metals Engineering Conference Detroit, October, 1968. To be published in Trans. ASM.

16. PARIS, P. C. 'The fracture mechanics approach to fatigue', Proc. Tenth Sagamore Army Materials Research Conference, August, 1963, Syracuse University Press, 1964.
17. WESSEL, E. T., CLARK, W. G., Jr. & WILSON, W. K. 'Engineering methods for the design and selection of materials against fracture', Available through DDC, AD801005. To be published by John Wiley and Sons, Inc.
18. TIFFANY, C. F. & HALL, L. R. 'Applications of sub-critical flaw growth data', presented at the National Symposium on Fracture Mechanics, Lehigh University, June 17-19, 1968. To be published in Engineering Fracture Mechanics, 1969.
19. TIFFANY, C. F. & MASTERS, J. N. 'Applied fracture mechanics', *ASTM STP 381*, p. 249, April, 1965.

Fig. 1
Dimensions and estimated measurement capacities of various sizes of compact tension specimens

Type	Estimated measurement capacity*		Tentative overall dimensions		
	K_{Ic}/σ_{ys}	$(K_{Ic}/\sigma_{ys})^2$	Thickness (in)	Height (in)	Width (in)
1T-CT	0·63	0·40	1	2·4	2·5
2T-CT	0·90	0·80	2	4·8	5·0
3T-CT	1·10	1·20	3	7·2	7·5
4T-CT	1·30	1·60	4	9·6	10·0
6T-CT	1·60	2·40	6	14·4	15·0
8T-CT	1·80	3·20	8	19·2	20·0
10T-CT	2·00	4·00	10	24·0	25·0
12T-CT	2·20	4·80	12	28·8	30·0

* Based on currently suggested ASTM E-24 minimum size criterion a and $B \geqq 2{\cdot}5\ (K_{Ic}/\sigma_{ys})^2$. (Ref. 5 & 8).

Fig. 3
*Chemical compositions and typical heat treatments for alloys investigated**

Type steel	Chemical composition Wt. % max. unless otherwise noted									
	C	Mn	P	S	Si	Ni	Cr	Mo	V	Cu
A533 Gr.B Class I	0·25	1·15/ 1·50	1·10/ 1·55	0·035	0·15/ 0·30	0·40/ 0·70	–	0·45/ 0·60	–	–
A216 WCC	0·25	1·20	0·05	0·06	0·60	0·50	0·40	0·25	–	0·50
A469 CL-4	0·27	0·70	0·015	0·018	0·15/ 0·30	3·0 Min.	0·50	0·20/ 0·60	0·03 Min.	–
A470 CL-8	0·25/ 0·35	1·00	0·015	0·018	0·15/ 0·30	0·75	0·90/ 1·5	1·0/ 1·5	0·20/ 0·30	–
A471 CL-5	0·28	0·60	0·015	0·018	0·10	3·25/ 4·0	1·25/ 2·0	0·30/ 0·60	0·05/ 0·15	

Type steel	Typical heat treatment			
	Normalized	Austenitized	Tempered	Stress relieved
A533 Gr.B Class I		1550°F for 4 hours, water quenched	1225°F ± 25°F – ½ hr. for 1 in thickness	1135°F ± 25°F, 25 hr., Furnace cool to 600°F, air cool to room temp.
A215 WCC	Double normalized at 1650°F and 1750°F for 8 hours		1200°F for 8 hours	
A469 CL-4	1700°F for 30 hours	1480°F for 30 hours, water quenched	1160°F for 30 hours, air cooled	1125°F for 30 hours furnace cooled
A470 CL-8	1850°F for 30 hours	1750°F for 30 hours, air cooled	1225°F for 30 hours, air cooled	1175°F for 30 hours, furnace cooled
A471 CL-5	1750°F for 30 hours	1550°F for 30 hours, water quenched	1120°F for 30 hours air cooled	1075°F for 30 hours, furnace cooled

* Values taken from ASTM specifications.

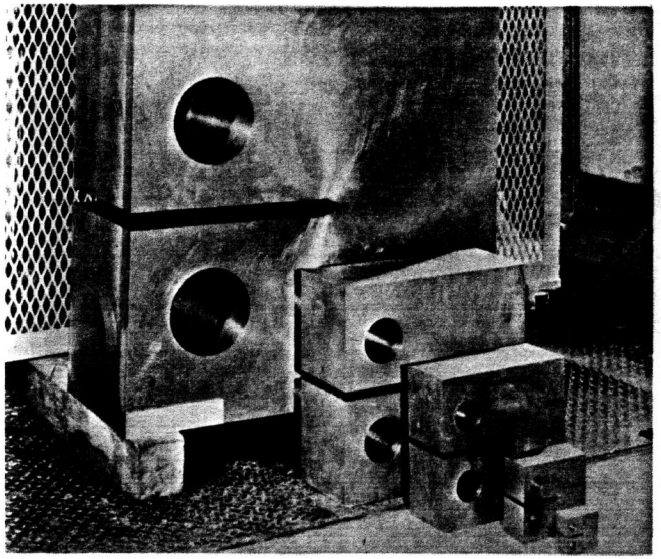

Fig. 2. Compact tension fracture toughness specimens (1, 2, 4, 6 and 12 in thick).

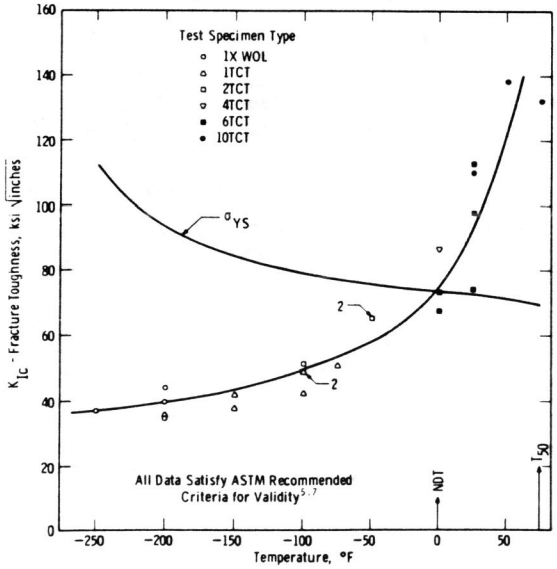

Fig. 5. Temperature dependence of K_{Ic} fracture toughness for A533B steel (12 in thick plate).

Fig. 4
*Tensile and impact properties of alloys investigated**

	Room temperature tensile properties				Impact properties	
Type steel	*0·20% Yield strength ksi*	*Tensile strength ksi*	*Elongation %*	*Reduction in area %*	*FATT °F*	*NDT °F*
A533 Gr.B,Cl. I	50·0 min	80·0 to 100·0	16	63	95	–
A216 WCC	40·0 min	70·0	22	35	90	–
A469 CL-4	85·0 to 95·0	100·0 to 110·0	18 to 20	45 to 60	50 to 100	0 to 50
A470 CL-8	85·0 to 95·0	105·0 to 120·0	15 to 18	40 to 50	150 to 225	125 to 150
A471 CL-5	120·0 to 130·0	135·0 to 145·0	16 to 18	40 to 50	−50 to 0	−100 to 75

* Values taken from ASTM specifications.

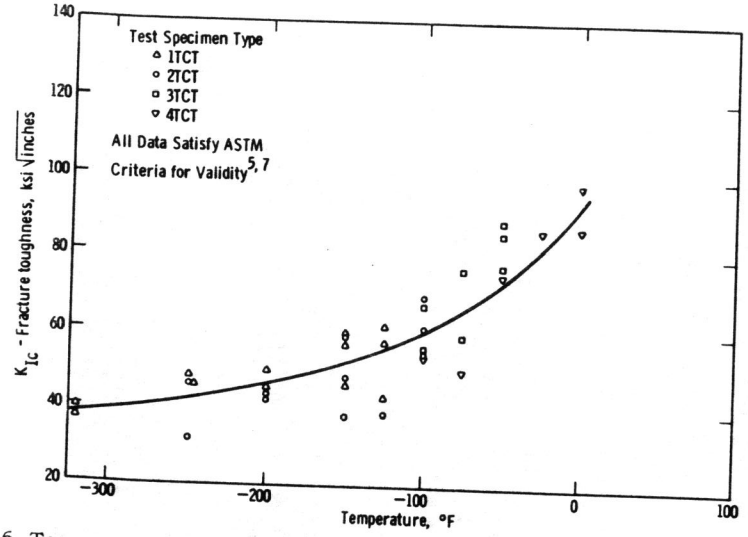

Fig. 6. Temperature dependence of K_{Ic} fracture toughness for A533-B steel (11¾ in thick plate).

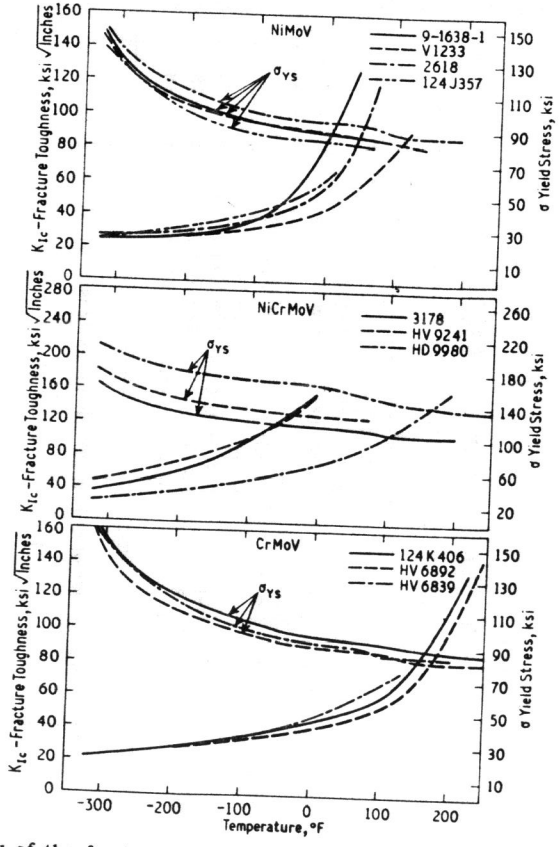

Fig. 7. Summary of the fracture toughness behavior of various forgings for the three alloy types.

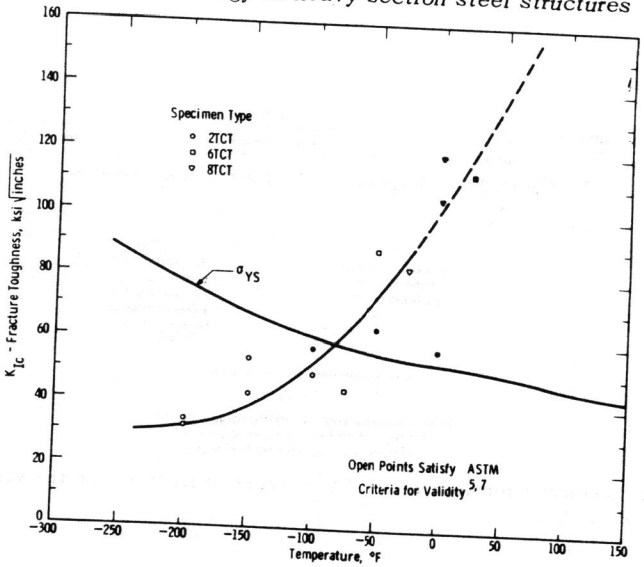

Fig. 8. Temperature dependence of yield strength and K_{Ic} fracture toughness for A216-C cast steel.

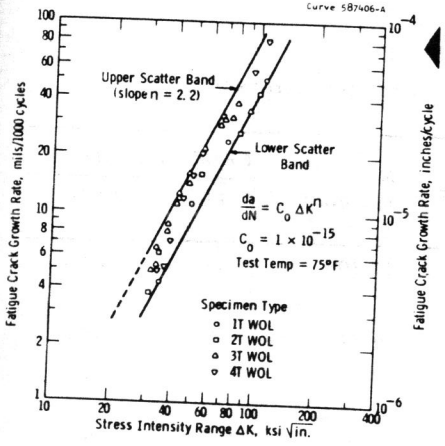

Fig. 9. Fatigue crack growth rate as a function of ΔK for A533-B steel.

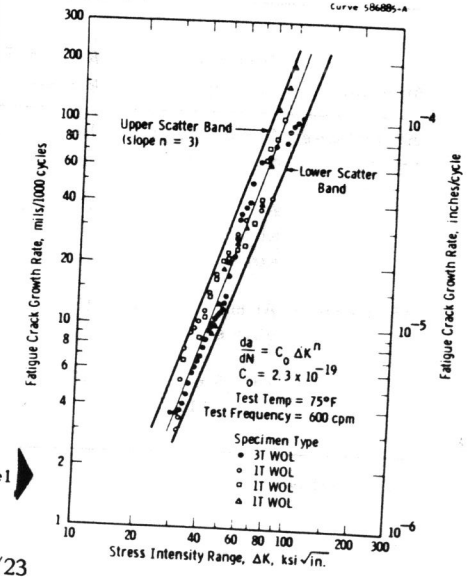

Fig. 10. Fatigue crack growth rate as a function of ΔK for A216-C cast steel keel block.

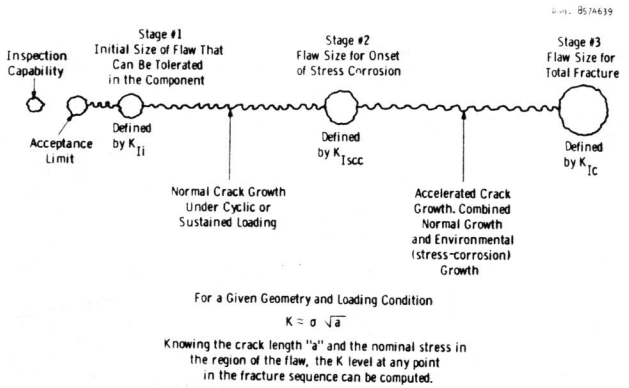

Fig. 11. Schematic representation of the stages of fracture and the various defect sizes involved.

Fig. 13
Critical flaw sizes at 75°F for various operating stresses

Material	*Operating conditions*	K_{Ic}@75°F ksi $\sqrt{in}$	*Max. operating stress, psi*	*Critical flaw size*	
				Depth, in	*Length, in*
A216-C Cast Steel	At max. allowable stress*	155	23,300	12·20	122·0
	At 1·5 max. allowable stress	155	35,000	4·92	49·2
A533B Steel	At max. allowable stress	130	26,700	6·57	65·7
	At 1·5 max. allowable stress	130	40,000	2·67	26·7

* Code allowable.

Fig. 12
Critical flaw sizes at 75°F for various proof testing conditions

Material	*Minimum yield strength, psi*	K_{Ic} @ 75°F ksi $\sqrt{in}$	*Proof test conditions*	*Proof test stress*	*Critical flaw size*	
					depth, in	*length, in*
A216 C Cast Steel	40,000	155	1·25 × max. design stress	29,100	7·44	74·4
	40,000	155	0·9 × σ_{ys}	36,000	4·40	44·0
	40,000	155	1·35 × σ_{ys}	54,000	1·58	15·8
A533 B Steel	50,000	130	1·25 × max. design stress	33,300	4·00	40·0
	50,000	130	0·9 × σ_{ys}	45,000	2·00	20·0
	50,000	130	1·35 × σ_{ys}	67,500	0·71	7·1

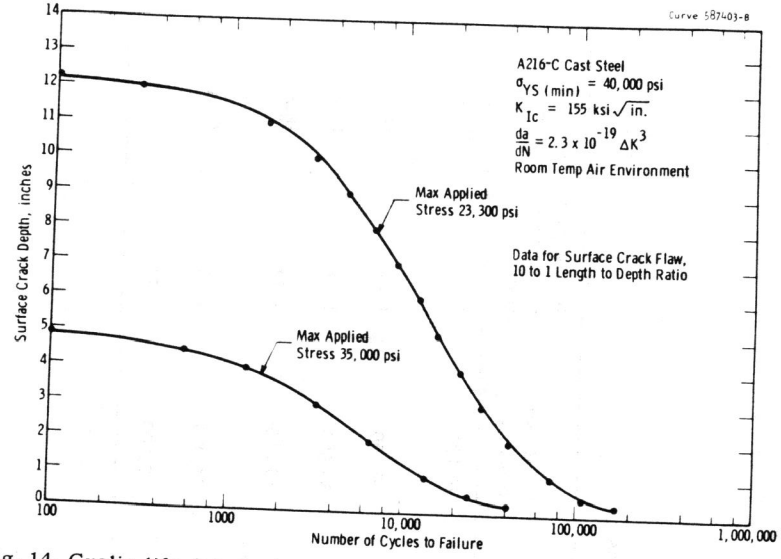

Fig. 14. Cyclic life data for hypothetical example problem involving A216-C cast steel.

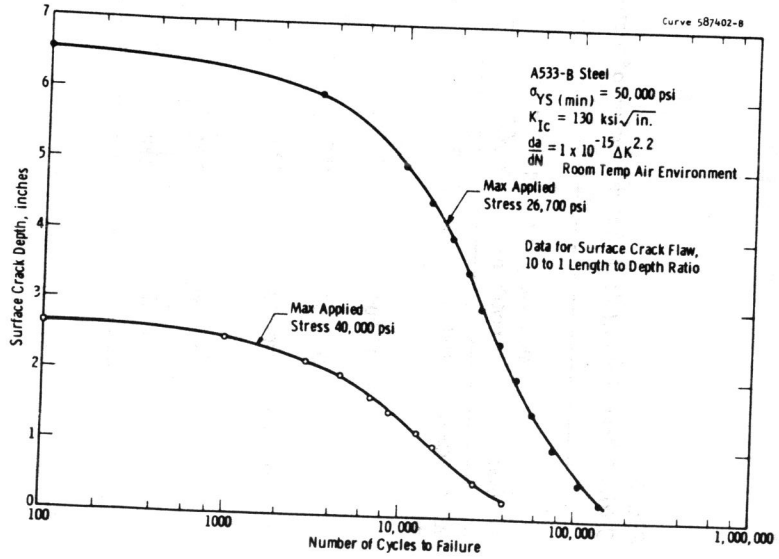

Fig. 15. Cyclic life data for hypothetical example problem involving A533-B steel.